FOXO1 in the ventromedial hypothalamus regulates energy balance

Ki Woo Kim,[1,2] Jose Donato Jr.,[1] Eric D. Berglund,[1,2] Yun-Hee Choi,[1] Daisuke Kohno,[1,2] Carol F. Elias,[1] Ronald A. DePinho,[3] and Joel K. Elmquist[1,2]

[1]Division of Hypothalamic Research, Department of Internal Medicine, and [2]Department of Pharmacology, The University of Texas Southwestern Medical Center (UT Southwestern), Dallas, Texas, USA. [3]Department of Cancer Biology, The University of Texas MD Anderson Cancer Center, Houston, Texas, USA.

The transcription factor FOXO1 plays a central role in metabolic homeostasis by regulating leptin and insulin activity in many cell types, including neurons. However, the neurons mediating these effects and the identity of the molecular targets through which FOXO1 regulates metabolism remain to be defined. Here, we show that the ventral medial nucleus of the hypothalamus (VMH) is a key site of FOXO1 action. We found that mice lacking FOXO1 in steroidogenic factor 1 (SF-1) neurons of the VMH are lean due to increased energy expenditure. The mice also failed to appropriately suppress energy expenditure in response to fasting. Furthermore, these mice displayed improved glucose tolerance due to increased insulin sensitivity in skeletal muscle and heart. Gene expression profiling and sequence analysis revealed several pathways regulated by FOXO1. In addition, we identified the nuclear receptor SF-1 as a direct FOXO1 transcriptional target in the VMH. Collectively, our data suggest that the transcriptional networks modulated by FOXO1 in VMH neurons are key components in the regulation of energy balance and glucose homeostasis.

Introduction

Defective regulation of energy balance results in obesity and components of metabolic syndrome, such as type 2 diabetes. Understanding the molecular and cellular mechanisms underlying the ability of the central nervous system to regulate energy balance and glucose homeostasis is an area of active investigation. Many proteins are involved in the modulation of metabolic homeostasis. This includes the transcription factor FOXO1, which has been demonstrated to regulate leptin and insulin action in the brain (1, 2). The biological significance of mammalian FOXO1 was initially reported in studies in *Caenorhabditis elegans*. Two independent groups identified *Daf-16* (a homolog of the mammalian FOXO1) as a negative regulator of *Daf2* (a homolog of the mammalian insulin receptor) signaling in *C. elegans*, implying that FOXO1 may play important roles in insulin signaling (3, 4). Subsequent studies using mouse models have confirmed the functional significance of FOXO1 as a critical mediator of insulin effects in many mammalian peripheral cells (1, 5, 6).

Recently, critical metabolic roles of FOXO1 in the hypothalamus have been reported (2, 7). Both studies assessed the role of FOXO1 in melanocortin neurons in the arcuate nucleus of the hypothalamus (ARH). Specifically, they reported *POMC* and *Agrp* genes as direct targets of FOXO1. A subsequent report using POMC-specific FOXO1 KO mice demonstrated that FOXO1 plays important roles in regulation of food intake, body weight, and leptin sensitivity, partially depending on the expression of carboxypeptidase E (*Cpe*) (8). Furthermore, analyses of PDK1/FOXO1 pathways revealed critical roles of FOXO1 to control food intake, body length, and body weight in AGRP neurons of hypothalamus (9).

FOXO1 is also highly expressed in many other hypothalamic nuclei, including the dorsomedial nucleus of the hypothalamus and the ventral medial nucleus of the hypothalamus (VMH) (2, 7). Several reports suggest that distinct neuronal populations are differentially regulated by key metabolic signals (10–12). However, the metabolic functions of FOXO1 in other hypothalamic neurons have yet to be delineated. Among several hypothalamic nuclei, the VMH has long been of interest as a site regulating body weight (2, 7, 8, 12–18). In addition, numerous recent studies have found that the upstream regulators of FOXO1, leptin and insulin, act in the VMH to regulate body weight homeostasis (7, 12, 15, 16, 19, 20).

Since FOXO1 is thought to play a prominent role in mediating the effects of leptin and insulin, we hypothesized that FOXO1 expressed by neurons in the VMH is a key molecular mediator of energy balance and glucose homeostasis. To directly address this question, we generated mice lacking FOXO1 in steroidogenic factor 1 (SF-1) neurons of the VMH (*Foxo1 KO^{Sf1}* mice) and investigated functional significance of FOXO1 in the VMH.

Results

VMH-specific FOXO1 deletion. To directly address potential roles of FOXO1 in the VMH, we generated SF-1 neuron-specific FOXO1-null (*Foxo1 KO^{Sf1}*) mice by crossing floxed *Foxo1* mice (21) and SF-1 Cre mice, which express Cre recombinase in subsets of neurons of the VMH (12). We successfully deleted FOXO1 in the VMH (Figure 1A). Allele-specific PCR showed deletion of FOXO1 in other tissues in which SF-1 is endogenously expressed, such as the pituitary gland, adrenal gland, and testis (Figure 1A). Other tissues examined, including the cerebellum and tail, did not show any Cre activity (Figure 1A). We also quantified FOXO1 levels using quantitative PCR (Q-PCR) in several tissues. We found significantly decreased expression of FOXO1 in the VMH, pituitary glands, and adrenal glands of *Foxo1 KO^{Sf1}* mice (Figure 1B). To further verify FOXO1 deletion in the VMH, we performed immunohistochemistry using a FOXO1-specific antibody (2). We detected FOXO1 immunoreactivity in several hypothalamic nuclei, including ARH, VMH, and dorsomedial nucleus of the hypothalamus in WT control mice, as described previously (2) (Figure 1, C and D). In contrast, FOXO1 immuno-

Conflict of interest: The authors have declared that no conflict of interest exists.
Citation for this article: *J Clin Invest.* 2012;122(7):2578–2589. doi:10.1172/JCI62848.

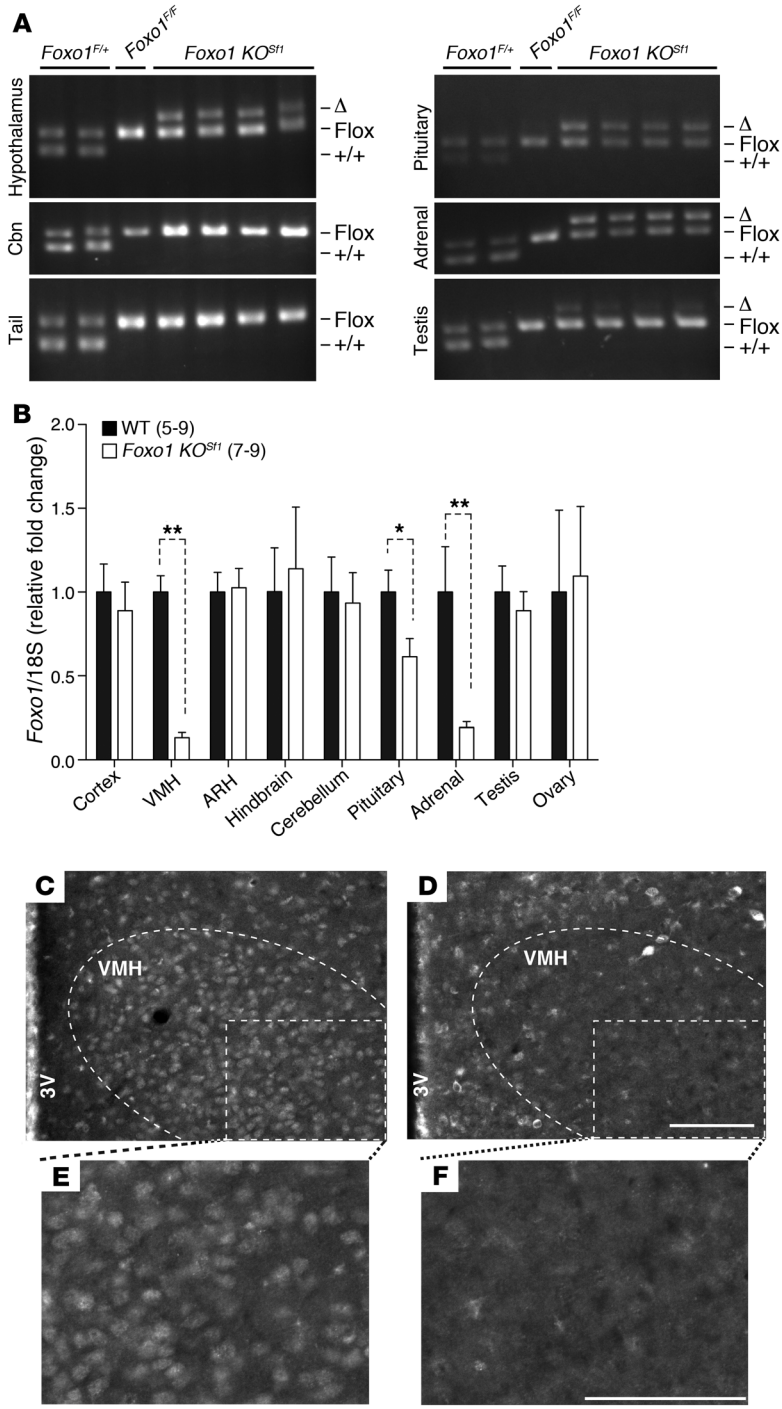

Figure 1
Validation of *Foxo1 KO*^{Sf1} mice. (**A**) PCR genotyping using hypothalami, cerebella, tails, pituitary glands, adrenal glands, and testes from *Foxo1*$^{F/+}$, *Foxo1*$^{F/F}$, and *Foxo1 KO*^{Sf1} mice. (**B**) Relative *Foxo1* expression in indicated tissues. Numbers of animals examined are expressed in parentheses. (**C** and **D**) Low-power view of FOXO1 immunostaining in mediobasal hypothalami of (**C**) WT and (**D**) *Foxo1 KO*^{Sf1} mice. (**E** and **F**) High-power view of FOXO1 staining indicated with white boxes in **C** and **D**. The data are expressed as mean ± SEM (*P < 0.01, **P < 0.0001, Student's t test). 3V, third ventricle. Cbn, cerebellum. Scale bar: 100 μm.

reactivity was reduced specifically in the VMH of *Foxo1 KO*^{Sf1} mice, confirming VMH-limited FOXO1 deletion (Figure 1, C–F).

Since SF-1 is expressed in the pituitary and adrenal glands and showed decreased expression of FOXO1 in tissues of *Foxo1 KO*^{Sf1} mice, we assessed the hypothalamic-pituitary-adrenal and hypothalamic-pituitary-gonadal axes of male mice. *Foxo1 KO*^{Sf1} mice displayed similar circulating follicle-stimulating hormone (FSH), luteinizing hormone (LH), testosterone, and corticosterone (normal and stressed) levels compared with those of control mice (Supplemental Table 1; supplemental material available online with this article; doi:10.1172/JCI62848DS1). Plasma triiodothyronine (T3) and thyroxine (T4) levels were also comparable between genotypes in fed and fasted states, suggesting an intact thyroid axis in *Foxo1 KO*^{Sf1} animals (Supplemental Table 1). In addition, the pituitary glands, adrenal glands, and testes of *Foxo1 KO*^{Sf1} mice were histologically indistinguishable from those of control mice (Supplemental Figure 1).

Leanness in Foxo1 KO^{Sf1} *mice*. Since FOXO1 plays important roles in leptin and insulin action in several sites and tissues, we examined the effects of FOXO1 deletion on the regulation of energy homeostasis. *Foxo1 KO*^{Sf1} mice showed comparable body length, regardless of food consumed (Supplemental Table 2). The body weight of chow-fed *Foxo1 KO*^{Sf1} mice was comparable to that of WT littermates until 10 weeks (male) and 7 weeks (female). Notably, body weights diverged thereafter, with the *Foxo1 KO*^{Sf1} mice becoming leaner (Figure 2, A and C). This lean phenotype was associated with decreased fat mass in both male and female mice (Figure 2, B and D). To assess the cause of lower body weight in *Foxo1 KO*^{Sf1} mice, we measured food intake, energy expenditure, and physical activity using metabolic chambers (20, 22, 23). These experiments were performed in weight-matched 5- to 7-week-old male mice prior to differences in body weight. *Foxo1 KO*^{Sf1} mice consumed the same cumulative and daily food intake as littermate controls (Figure 2, E and F). *Foxo1 KO*^{Sf1} mice also exhibited no differences in total movement compared with that of WT littermates (Figure 2H). However, *Foxo1 KO*^{Sf1} mice exhibited increased energy expenditure (Figure 2G). These results suggest that inactivation of FOXO1 in the VMH leads to a lean phenotype due to increased energy expenditure.

Effect of FOXO1 deletion in response to high-fat diet. Several genes, including the leptin receptor and the enzyme PI3K (*Pik3ca*), are known regulators of diet-induced obesity in the VMH (12, 15, 20, 23). Moreover, FOXO1 is highly expressed in the hypothalamus and plays critical roles in the leptin-induced PI3K/AKT pathway that modulates metabolic homeostasis (2, 24). We investigated the effect of FOXO1 deletion in the VMH during conditions of excess calorie intake. We fed male mice high-fat diet (HFD) starting at 5 weeks of age. Body weights were comparable between genotypes in male mice for the first 1–2 weeks after exposure to the

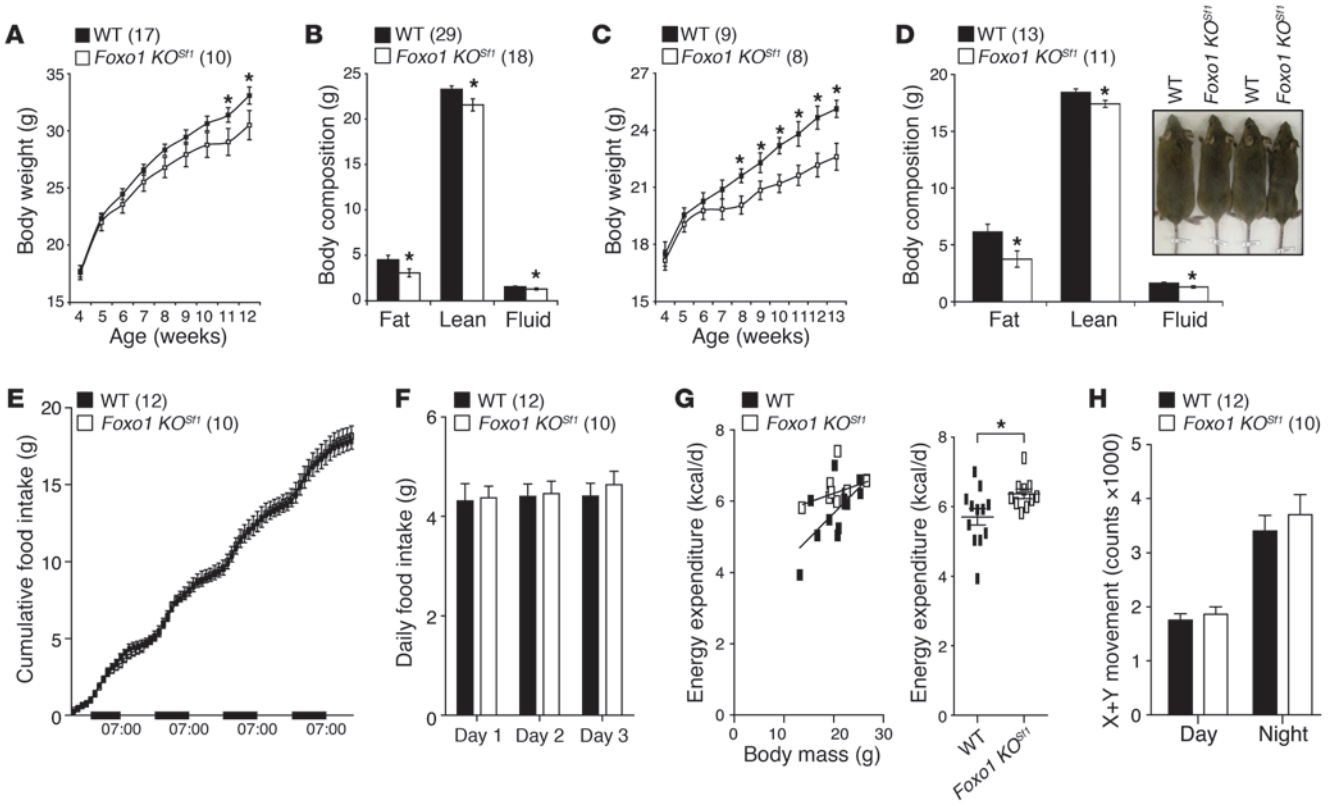

Figure 2

Phenotype of *Foxo1 KO*^{Sf1} mice. (**A**) Body weight of male mice fed with NC. (**B**) Body composition of male mice fed with NC aged 10–16 weeks. (**C**) Body weight of female mice fed with NC. (**D**) Body composition of female mice fed with NC aged 17–18 weeks. The inset shows a representative image of mice with the indicated genotypes. (**E**) Cumulative food intake, (**F**) daily food intake, (**G**) energy expenditure of individual mice, and (**H**) total movement (sum of movement on the X and Y axes) were measured. Numbers of animals examined are expressed in parentheses in each graph, and symbols in **G** represent individual mice. The data are expressed as mean ± SEM (**P* < 0.05, Student's *t* test). Counts, beam breaks counts.

HFD. Thereafter, *Foxo1 KO*^{Sf1} mice showed decreased body weight (Figure 3A). This resistance to diet-induced obesity shown in *Foxo1 KO*^{Sf1} mice was associated with decreased fat mass (Figure 3B). To understand this phenotype, body weight–matched, 5- to 6-week-old WT and *Foxo1 KO*^{Sf1} animals (21.53 ± 0.41 g and 20.73 ± 0.6 g, respectively; $P > 0.1$) were examined in metabolic cages during an acute change from regular chow to HFD. The respiratory exchange ratio (RER), movement, and food intake were comparable between genotypes. In contrast, the *Foxo1 KO*^{Sf1} mice exhibited markedly increased heat generation and O_2 consumption compared with that of WT littermates in response to HFD (Figure 3, C and D, and Supplemental Figure 2). Collectively, these results indicate that resistance to HFD shown in *Foxo1 KO*^{Sf1} mice is due mainly to increased thermogenic responses following exposure to HFD.

Thermogenesis induced by diet is mediated by the interscapular brown adipose tissue (iBAT) (18), and the VMH is a site in the brain that regulates sympathetic tone to iBAT (14, 17). In addition, activation of leptin signaling in the VMH induces activation of the sympathetic nervous system (SNS) and increased UCP1 expression in iBAT (25–27). UCP1 is well known to be a key regulator of thermogenesis in iBAT (28). Several studies have shown that impaired VMH function correlates with thermogenic defects in iBAT, including abnormal expression of UCP1 (20, 29, 30). We found that *Ucp1* mRNA was increased in iBAT from *Foxo1 KO*^{Sf1} mice (Figure 3E). Furthermore, the protein level of UCP1 was also more than 2-fold upregulated in iBAT of *Foxo1 KO*^{Sf1} mice (Figure 3, F and G). In addition to increased expression of UCP1 in iBAT, *Foxo1 KO*^{Sf1} mice had higher plasma norepinephrine levels than controls (Figure 3H). Epinephrine levels were not different (Figure 3H). These data suggest that the increased energy expenditure phenotype seen in *Foxo1 KO*^{Sf1} mice is due in part to increased SNS activity in *Foxo1 KO*^{Sf1} animals.

FOXO1 deletion in the VMH increases leptin sensitivity. The VMH is a key site for leptin action, and the activation of leptin signaling in the VMH, including SF-1 neurons, regulates energy homeostasis and SNS activation (2, 12, 15, 23, 24, 26, 27). FOXO1 acts as a negative regulator of leptin action in the hypothalamus (2, 7, 8). We hypothesized that deletion of FOXO1 in the SF-1 neurons may provide alteration of leptin sensitivity. To directly examine the effect of FOXO1 deletion in the VMH on leptin sensitivity, we administered leptin peripherally and monitored several metabolic parameters using indirect calorimetry. As expected, i.p. leptin injections reduced body weight in WT mice. Notably, leptin injections in *Foxo1 KO*^{Sf1} mice resulted in greater weight loss than those in controls (Figure 4A). Leptin inhibition of food intake was comparable between genotypes (Figure 4B). However, the *Foxo1 KO*^{Sf1} mice showed increased energy expenditure (Figure 4C). In addition, the RER was decreased in *Foxo1 KO*^{Sf1} mice after leptin

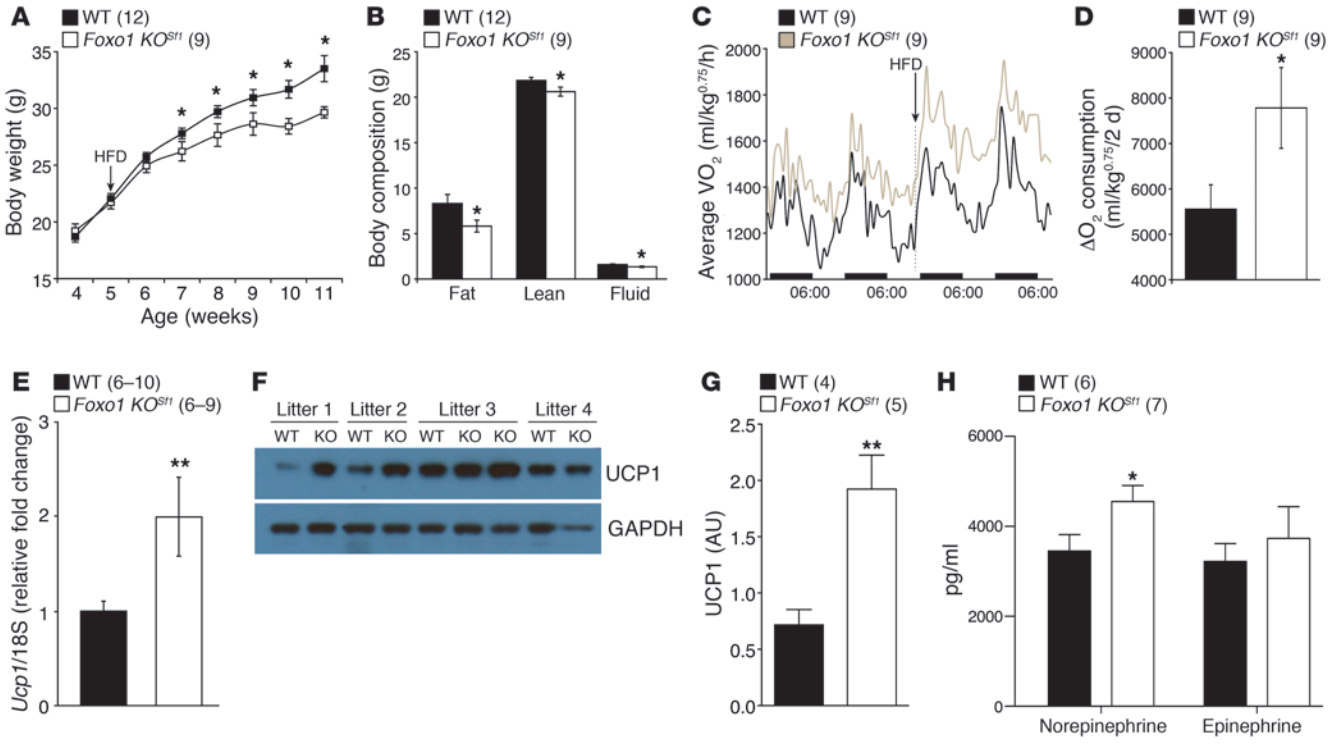

Figure 3

Effect of VMH-specific FOXO1 KO in body weight, UCP1 levels, and plasma catecholamines. (**A**) Body weight of male mice fed with HFD from 5 weeks. (**B**) Body composition (11–12 weeks old) of male mice fed HFD. (**C**) Temporal changes of O_2 consumption before and after the acute HFD challenge. (**D**) Changes in O_2 consumption before and after HFD. (**E**) *Ucp1* mRNA levels in iBAT from male mice fed NC (6–7 weeks old). (**F**) Individual UCP1 protein levels in iBAT of WT and *Foxo1 KO^{Sf1}* littermates (6–7 weeks old). (**G**) Average UCP1 protein levels in iBAT of WT and *Foxo1 KO^{Sf1}* counterparts (6–7 weeks old). (**H**) Plasma norepinephrine and epinephrine in chow-fed males (7–8 weeks old). Numbers of animals examined were expressed in parentheses in each graph. The data are expressed as either (**C**) average or mean ± SEM (*P < 0.05, **P < 0.01, Student's t test). WT, *Foxo1$^{F/F}$*; KO, *Foxo1 KO^{Sf1}*; Ucp, uncoupling protein.

injection, consistent with the hypothesis that increased leptin sensitivity preferentially facilitates fat utilization. Collectively, these results suggest that leptin-induced increases in energy expenditure may contribute to the greater body weight loss in *Foxo1 KO^{Sf1}* mice.

Fasting quickly reduces leptin levels, and falling levels of leptin act as a signal to the brain that starvation conditions exist and that appropriate responses need to be engaged (31). Leptin activates PI3K signaling and FOXO1 translocation in several hypothalamic sites, including the VMH neurons (2, 20, 32, 33). Thus, we assessed the physiological effects of FOXO1 deletion in VMH neurons following fasting. We fasted animals for 24 hours, measuring changes in body weight and energy expenditure using metabolic chambers. *Foxo1 KO^{Sf1}* mice lost substantially more weight than WT littermates after 24 hours of fasting (Figure 4D). This was due to higher energy expenditure in *Foxo1 KO^{Sf1}* mice during the fast (Figure 4E). We also noted a compensatory increase in energy intake in *Foxo1 KO^{Sf1}* animals during the refeeding period (Figure 4F). Collectively, these results suggest that FOXO1 in SF-1 neurons of the VMH is required to appropriately suppress energy expenditure during fasting.

Effect of FOXO1 deletion in the VMH on glucose metabolism and insulin action. The VMH is an important site for leptin and insulin signaling, and direct injection of leptin in the VMH has been shown to increase peripheral glucose uptake via activation of the SNS (12, 26, 34, 35). Based on our observations of increased plasma norepinephrine, increased leptin sensitivity, and increased expression of UCP1 in iBAT, we hypothesized that deletion of FOXO1 in the VMH modulates the SNS and ultimately changes insulin action and glucose metabolism. To address whether ablation of FOXO1 in the VMH impacts these parameters, we first measured fed and fasted blood glucose and plasma insulin levels. These measurements were performed in body weight–matched, 6- to 8-week-old mice. Plasma insulin levels were comparable between genotypes in both the fed and fasted condition (Figure 5B). However, blood glucose was lower in both fed and fasted *Foxo1 KO^{Sf1}* mice, suggesting improved insulin sensitivity (Figure 5, A and B). To further investigate the effect of FOXO1 deletion in the VMH on glucose homeostasis and insulin action, we performed glucose tolerance tests (GTTs) and insulin tolerance tests (ITTs). *Foxo1 KO^{Sf1}* mice exhibited improved glucose tolerance and insulin action compared with WT littermates (Figure 5, C and D). Collectively, these results suggest that FOXO1 signaling in the VMH modulates whole-body insulin action and glucose homeostasis.

FOXO1 in the VMH mediates insulin sensitivity in peripheral tissues. Hyperinsulinemic-euglycemic clamps were next performed to confirm greater insulin sensitivity in *Foxo1 KO^{Sf1}* mice. Importantly, mice used for these experiments were matched for body weight and body composition. Basal plasma insulin levels were similar and comparably elevated during the clamp (Figure 5E). Basal blood glucose was lower in *Foxo1 KO^{Sf1}* mice compared with that in WT controls, but this difference was normalized dur-

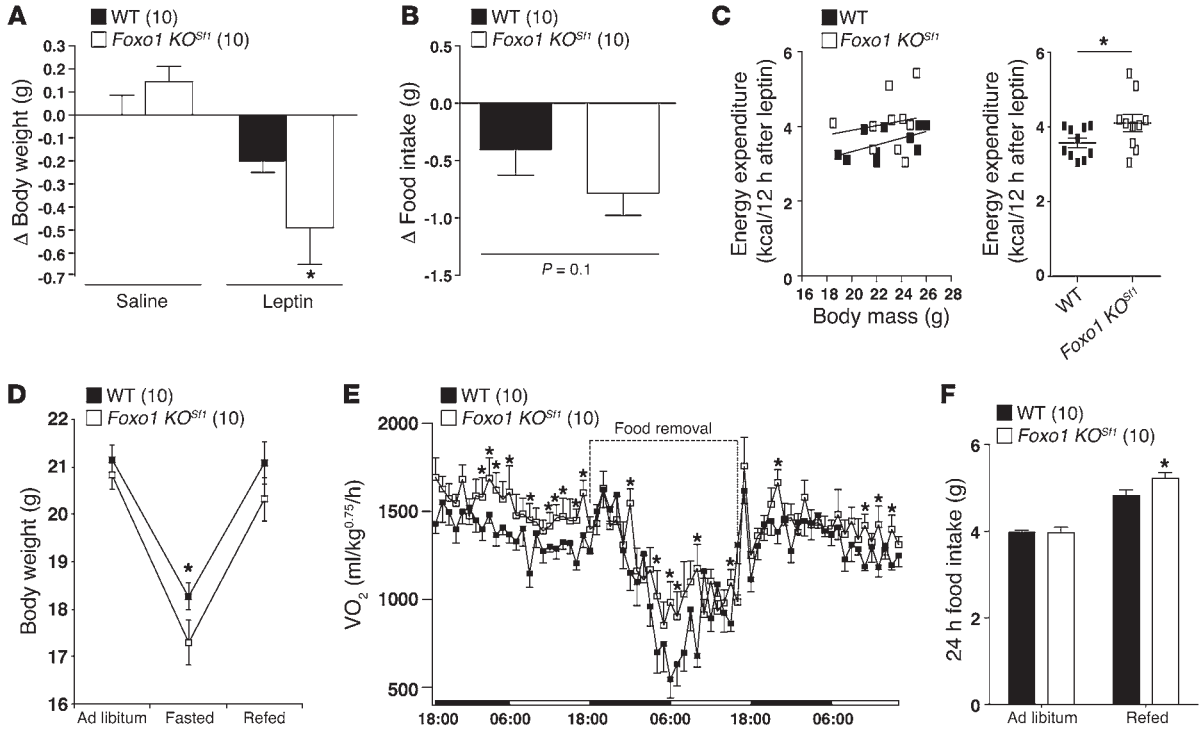

Figure 4
Effect of FOXO1 KO in the VMH on leptin administration and fasting. (**A**) Changes in body weight after exogenous leptin injection (significant leptin effect [2-way ANOVA, $F_{1,34} = 5.02$]). (**B**) Changes in food intake after exogenous leptin administration. (**C**) Energy expenditure for individual mice for 12 hours after leptin injection. Symbols represent individual mice. (**D**) Changes in body weight during fasting and refeeding. (**E**) Temporal changes of VO_2 before and after fasting (significant interaction between genotype and time (2-way ANOVA, $F_{69,1260} = 1.33$, $P = 0.0381$). (**F**) Food intake for 24 hours during ad libitum or refeeding. Numbers of animals used are expressed in parentheses in each graph. The data are expressed as mean ± SEM (*$P < 0.05$, Student's *t* test).

ing the clamp (Figure 5F). The exogenous glucose infusion rate (GIR) needed to maintain clamp blood glucose at similar levels was increased in *Foxo1 KO^{Sf1}* mice compared with that in WT controls, indicating greater whole-body insulin action (Figure 5G). Tracer dilution techniques revealed that basal endogenous glucose production (endoR_a) and glucose disposal rates (R_d) were similar between groups (Figure 5, H and I). Insulin-mediated suppression of endoR_a was also similar between groups during the clamp (Figure 5H). In contrast, hyperinsulinemia stimulated a marked increase in R_d in *Foxo1 KO^{Sf1}* mice compared with that in WT controls (Figure 5I). To further understand this increment in peripheral insulin sensitivity, we examined tissue-specific glucose uptake (R_g) using a bolus injection of 2-[^{14}C]deoxyglucose (2-DG) during the clamp. R_g in heart and gastrocnemius muscle was higher in *Foxo1 KO^{Sf1}* mice compared with that in WT controls (Figure 5J). There was also a trend indicating that insulin-stimulated R_g was greater in the soleus of *Foxo1 KO^{Sf1}* mice (Figure 5J). In contrast, R_g in white adipose tissue (WAT) was similar between genotypes (Figure 5J). Taken together, these results demonstrate that insulin-stimulated glucose disposal is enhanced in cardiac and skeletal muscle of *Foxo1 KO^{Sf1}* mice, and these differences likely contribute to lowered blood glucose.

FOXO1 directly regulates SF-1 expression in the VMH. Since SF-1 neurons of the VMH are critical targets of leptin and insulin action and the *Foxo1 KO^{Sf1}* mice displayed a marked increase in energy expenditure, we expected that several genes regulating diet-induced thermogenesis might be changed in neurons lacking FOXO1 in the VMH (12, 15, 20, 36, 37). Gene expression profiling revealed changes in a number of metabolic regulatory pathways (Figure 6A). Interestingly, nuclear receptor signaling pathways were broadly modulated, including the expression of SF-1 (Figure 6, A and B). SF-1 is a nuclear receptor expressed only in the VMH and is known to play a role in regulation of diet-induced thermogenesis (23). SF-1 levels were significantly elevated in the VMH of 24-hour–fasted *Foxo1 KO^{Sf1}* mice compared with those in WT littermates (Figure 6B). Sequence analyses revealed 3 putative FOXO1 binding sites in the SF-1 proximal promoter region, which are located tandemly, and the putative binding sequences were highly conserved between mammals (Figure 6C).

We next assessed whether the FOXO1 could directly bind to the promoter region of SF-1 and regulate its activity in the VMH. We used a ChIP assay using 2 different antibodies specific for FOXO1 (2, 7) and found that FOXO1 binds to the SF-1 promoter region (Figure 6D). In addition, we used a luciferase reporter assay and found that the WT FOXO1 and constitutively nuclear FOXO1 suppressed the SF-1 expression dose-dependently. This effect was observed in a –240 mSF-1-luc construct, but this effect was absent in a –80 mSF-1-luc construct (Figure 6, C, E, and F). Notably, a DNA binding-deficient FOXO1 could not repress SF-1 promoter activity (Figure 6F). Finally, *Foxo1 KO^{Sf1}* mice fasted for 24 hours exhibited increased SF-1 protein in the VMH (Figure 6, G and H). Taken together, these results lead to the prediction that FOXO1

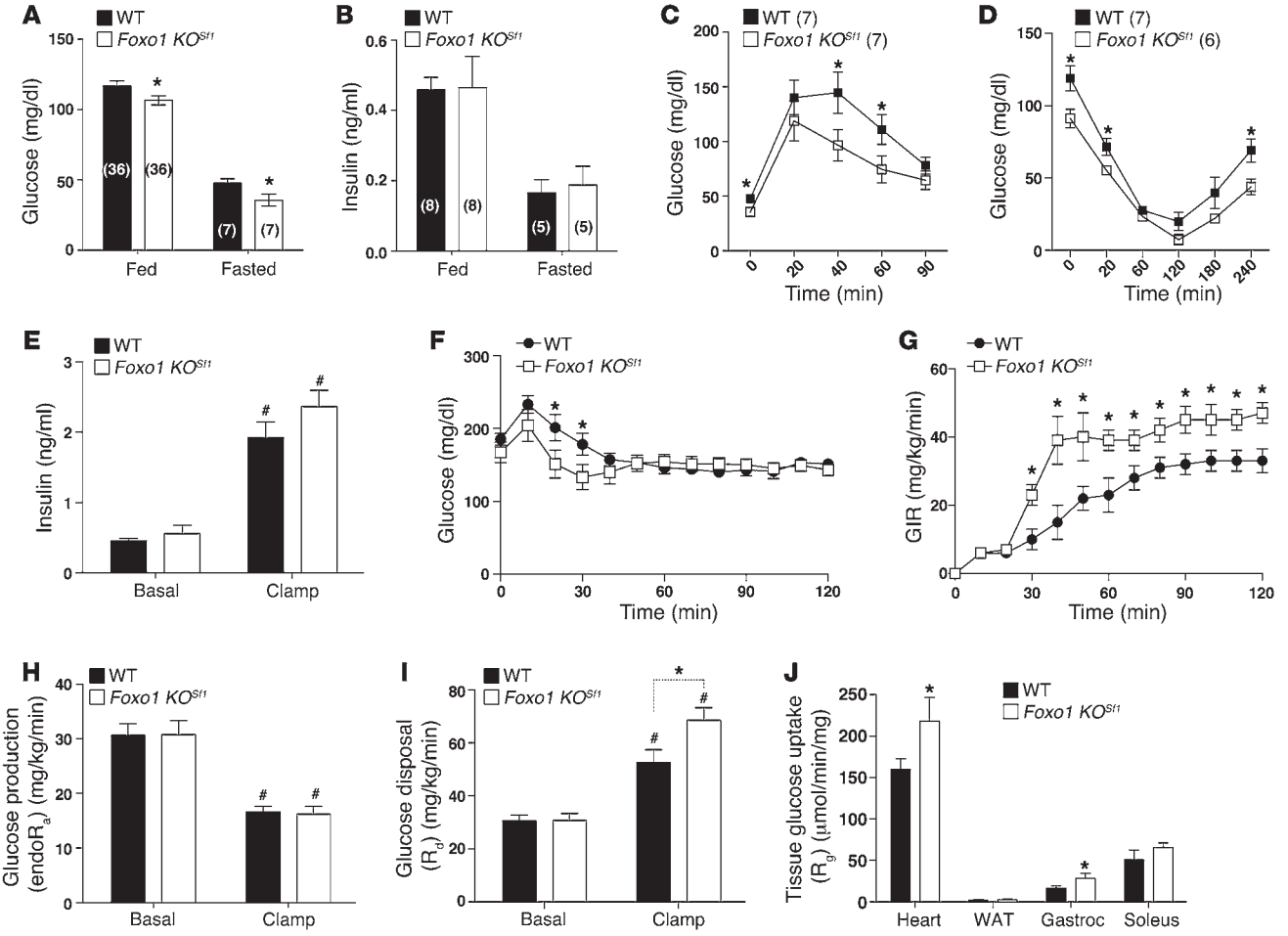

Figure 5

Glucose and insulin homeostasis in WT and *Foxo1 KO*^{Sf1} mice. (**A**) Glucose and (**B**) insulin levels of WT and *Foxo1 KO*^{Sf1} mice in fed and fasted states. (**C**) GTT (significant genotype effect [2-way ANOVA, $F_{1,60} = 10.5$, $P = 0.002$]). (**D**) ITT (significant genotype effect [2-way ANOVA, $F_{1,66} = 22.22$, $P < 0.0001$]). (**E**) Basal and clamped insulin, (**F**) blood glucose, (**G**) GIR, (**H**) hepatic EndoR$_a$, (**I**) R$_d$, and (**J**) tissue R$_g$ in WT and *Foxo1 KO*^{Sf1} mice ($n = 8$ for each genotype). The data are expressed as mean ± SEM (*$P < 0.05$, #$P < 0.01$, Student's *t* test). Gastroc, gastrocnemius muscle; Soleus, soleus muscle.

acts as a transcriptional suppressor of SF-1 expression and, absence of this regulation by deletion of FOXO1, may increase SF-1 activity in the VMH, leading to increased energy expenditure (23).

Deletion of SF-1 in the VMH impairs glucose homeostasis. Ablation of FOXO1 in SF-1 neurons produces a lean phenotype and improved whole-body glucose homeostasis. We previously found that SF-1 deletion results in an opposite phenotype that includes obesity that is due to decreased energy expenditure following exposure to HFD. Consistent with these in vivo observations, our in vitro data suggest that FOXO1 exerts a negative effect on SF-1 expression in the VMH. We hypothesized that transcriptional networks regulated by SF-1 in VMH neurons are necessary for normal glucose homeostasis. To test this hypothesis, we used mice with postnatal VMH-specific deletion of SF-1 (*Sf1 KO*$^{ckIICre;F/F}$ mice) (23). We first measured fed and fasted glucose levels in chow-fed, body weight–matched *Sf1 KO*$^{ckIICre;F/F}$ mice and WT littermates. *Sf1 KO*$^{ckIICre;F/F}$ mice showed higher fed blood glucose levels, suggesting impaired glucoregulation (Figure 7A). To further investigate the effect of SF-1 deletion in the VMH on glucose homeostasis and insulin action, we performed GTTs and ITTs. *Sf1 KO*$^{ckIICre;F/F}$ mice exhibited reduced glucose tolerance and insulin action compared with that of littermate controls (Figure 7, B and C). These results indicate that SF-1 signaling in the VMH is required for appropriate whole-body insulin action and glucose homeostasis.

To delineate underlying mechanisms on altered glucose/insulin homeostasis, hyperinsulinemic-euglycemic clamp studies were performed. As in the previous experiments, we used age- and body weight–matched littermates to avoid complications interpreting these data. Basal plasma insulin levels were similar and comparably elevated during the clamp (Figure 7D). Basal blood glucose, as expected, was higher in *Sf1 KO*$^{ckIICre;F/F}$ mice, but this difference was normalized during the clamp (Figure 7E). The GIR in *Sf1 KO*$^{ckIICre;F/F}$ mice was decreased compared with that in WT controls, indicating lower whole-body insulin action (Figure 7F). Basal endoR$_a$ and R$_d$ were similar between groups (Figure 7, G and H). Insulin-mediated suppression of endoR$_a$ was also similar between groups during the clamp (Figure 7G). In contrast, insulin-stimulated glucose disposal was lower in *Sf1 KO*$^{ckIICre;F/F}$ mice com-

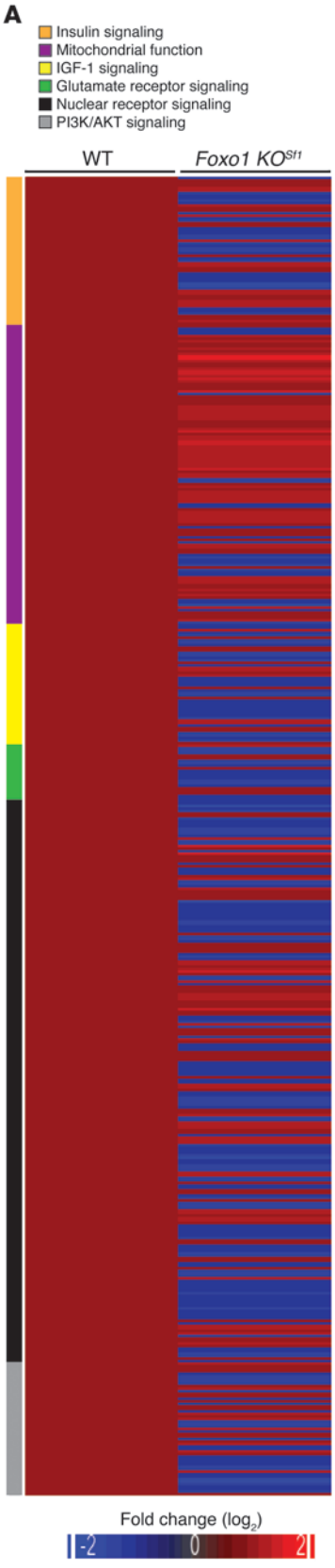
A
Insulin signaling
Mitochondrial function
IGF-1 signaling
Glutamate receptor signaling
Nuclear receptor signaling
PI3K/AKT signaling
WT
Foxo1 KOSf1
Fold change (log2)
-2
0
2

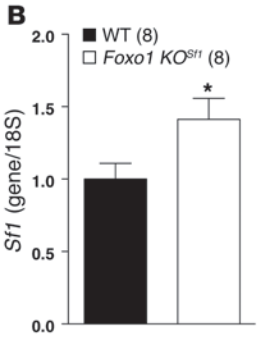
B
WT (8)
Foxo1 KOSf1 (8)
Sf1 (gene/18S)
2.0
1.5
1.0
0.5
0.0
*

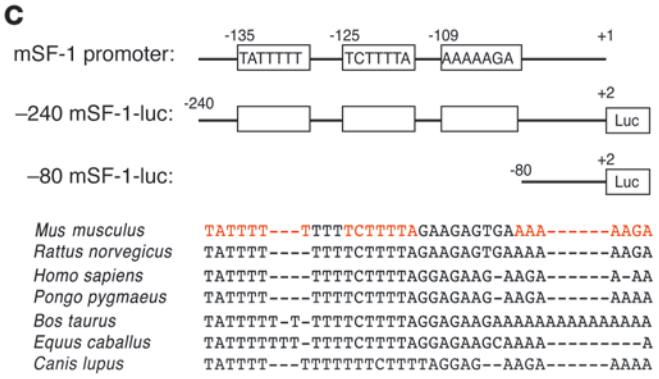
C
mSF-1 promoter:
-135
-125
-109
+1
TATTTTT
TCTTTTA
AAAAAGA
–240 mSF-1-luc:
-240
+2
Luc
–80 mSF-1-luc:
-80
+2
Luc
Mus musculus TATTTT---TTTTTCTTTTTAGAAGAGTGAAAA------AAGA
Rattus norvegicus TATTTT----TTTTCTTTTAGAAGAGTGAAAA------AAGA
Homo sapiens TATTTT----TTTTCTTTTAGGAGAAG-AAGA------A-AA
Pongo pygmaeus TATTTT----TTTTCTTTTAGGAGAAG-AAGA------AAAA
Bos taurus TATTTTT-T-TTTTCTTTTAGGAGAAGAAAAAAAAAAAAAAA
Equus caballus TATTTTTTT-TTTTCTTTTAGGAGAAGCAAAA---------A
Canis lupus TATTTT---TTTTTTTCTTTTAGGAG--AAGA------AAAA

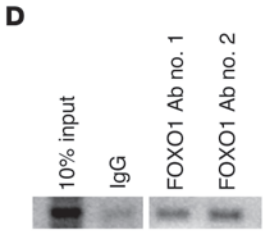
D
10% input
IgG
FOXO1 Ab no. 1
FOXO1 Ab no. 2

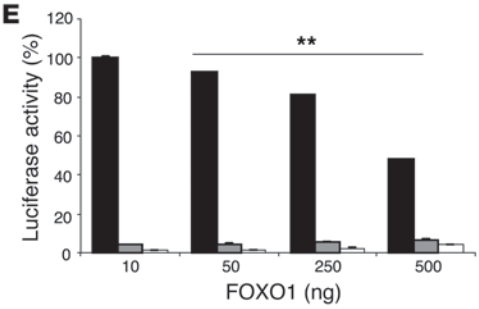
E
Luciferase activity (%)
120
100
80
60
40
20
0
**
10
50
250
500
FOXO1 (ng)

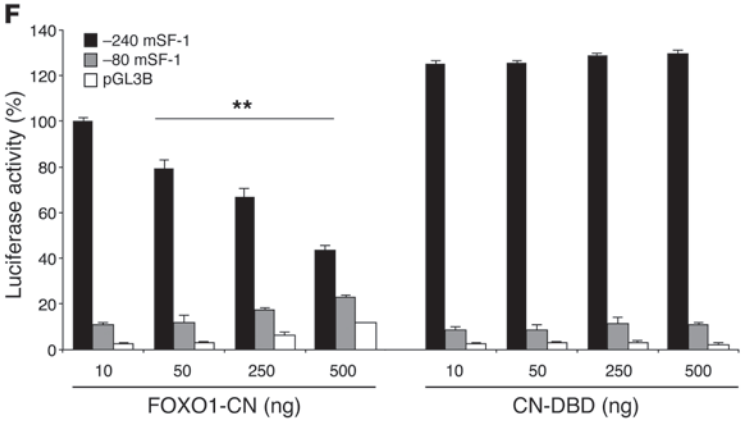
F
–240 mSF-1
–80 mSF-1
pGL3B
Luciferase activity (%)
140
120
100
80
60
40
20
0
**
10
50
250
500
FOXO1-CN (ng)
10
50
250
500
CN-DBD (ng)

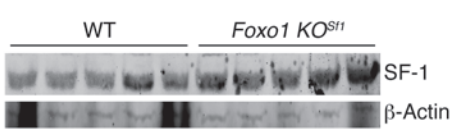
G
WT
Foxo1 KOSf1
SF-1
β-Actin

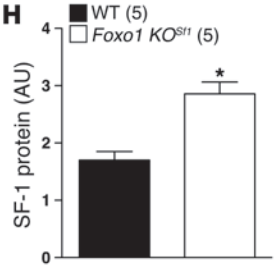
H
WT (5)
Foxo1 KOSf1 (5)
SF-1 protein (AU)
4
3
2
1
0
*

Figure 6
Transcriptional regulation of FOXO1 in the VMH. (**A**) Heat map demonstrating gene expression profiling in the VMH of WT and *Foxo1 KO^{Sf1}* mice. Relative fold changes of genes involved in indicated signaling pathways are shown (WT value = 1). (**B**) *Sf1* mRNA levels in the VMH of 24-hour–fasted WT and *Foxo1 KO^{Sf1}* mice (*P < 0.05, *t* test). (**C**) Schematic diagram of the 5′-flanking region of the mouse *Sf1* gene, including the location of potential FOXO1 binding sites (white boxes). Shown below are the 5′-deletion constructs. Genomic alignments of SF-1 5′-flanking region of mammals (around FOXO1 putative binding sites). Red indicates the putative FOXO1 binding sites. (**D**) ChIP analysis showing direct binding of FOXO1 on the SF-1 promoter region in the VMH. (**E**) SF-1 promoter activity is significantly repressed by FOXO1 in Neuro2A cells in a dose-dependent manner (**P < 0.0001, only for –240 mSF-1, 1-way ANOVA). (**F**) SF-1 promoter activity is significantly repressed by a constitutive nuclear active form of FOXO1 (FOXO1-CN) in a dose-dependent manner but not by a DNA-binding deletion mutant of FOXO1 (CN-DBD) in Neuro2A cells (**P < 0.0001, only for –240 mSF-1, 1-way ANOVA). (**G** and **H**) SF-1 protein levels in 24-hour–fasted WT and *Foxo1 KO^{Sf1}* animals (*P < 0.05, *t* test). The data are expressed as mean ± SEM (**B**, **E**, **F**, and **H**).

pared with that in WT controls, demonstrating impaired insulin sensitivity in peripheral (extrahepatic) tissues (Figure 7H). This conclusion is reinforced by lowered R_g in BATs and soleus muscles of *Sf1 KO$^{ckIICre;F/F}$* mice (Figure 7I). R_g in the heart, WAT, vastus lateralis, and gastrocnemius muscle was comparable between genotypes (Figure 7I). Collectively, these results further support the model that FOXO1- and SF-1–dependent networks in the VMH play important roles in regulating whole-body insulin action and glucose homeostasis.

Discussion

Obesity is associated with many metabolic disorders, including type 2 diabetes, dyslipidemia, and cardiovascular disease. The hypothalamus is a critical brain site regulating body weight, energy balance, and modulating glucose homeostasis. Therefore, understanding molecular mechanisms responsible for body weight regulation and glucose homeostasis in the hypothalamus will provide strategies to develop pharmacological intervention to combat metabolic disorders. Collectively, our results provide additional evidence demonstrating a role for SF-1 neurons and related transcriptional programs to regulate energy expenditure. Our results also add FOXO1 (and gene programs regulated by FOXO1 in SF-1 neurons) to the growing list of factors regulating energy balance. We have found that FOXO1 in neurons in the VMH also regulates glucose homeostasis. FOXO1 ablation in VMH SF-1 neurons increases energy expenditure without changing food intake, resulting in a lean phenotype. Moreover, ablation of FOXO1 in SF-1 neurons results in mice that are resistant to HFD-induced obesity, which is due to increased energy expenditure. Mice lacking FOXO1 in SF-1 neurons lose more weight following leptin administration due to increased energy expenditure. At the other end of the energy balance spectrum, we have found that VMH-specific FOXO1 KO mice lose more weight during a fast, a response that is due to a failure to appropriately suppress energy expenditure.

We also identified the *Sf1* gene itself as a putative target of FOXO1 in the VMH. Our results predict that suppression of SF-1 during a fast is due in part to direct binding of FOXO1 to the SF-1 promoter. Further, these data are consistent with a model in which falling levels of leptin and insulin during a fast result in less activation of PI3K activity and more nuclear accumulation of FOXO1 and lower levels of SF-1. This regulation of SF-1 is required for appropriate modulation of energy expenditure in the face of changing levels of energy availability. Thus, identification of key downstream transcriptional programs of SF-1 and FOXO1 in SF-1 neurons may provide insights into potential targets that affect energy expenditure without changing food intake.

This study proposes the involvement of the transcription factor FOXO1 in regulation of energy expenditure in the VMH. Upon activation by metabolic stimuli such as leptin and insulin in the VMH of the WT animals, FOXO1 will be phosphorylated by the activated PKB (pAkt) and excluded from the nucleus, ultimately leading actions of leptin and insulin. Since FOXO1 has been known as a negative regulator of the leptin/PI3K/pAkt signaling pathway, FOXO1 removal from the VMH may confer permanently increased sensitivity to leptin in the nucleus and may preferentially induce alternations in neuronal activity and regulation of downstream target genes. In addition, increased levels of plasma norepinephrine and elevated UCP1 levels in iBAT of *Foxo1 KO^{Sf1}* animals suggest that inhibition of FOXO1 in the SF-1 neurons of the VMH leads to activation of the SNS. This is consistent with several previous studies that have shown that leptin activates the SNS in mammals through increased catecholamine output (25, 38). Moreover, leptin injections into the VMH induced *Ucp1* mRNA levels through activation of the SNS (25–27). These results support the notion that leptin action on the regulation of the SNS in the VMH may preferentially be mediated by PI3K/AKT/FOXO1 pathways rather than Jak/Stat3 pathways (24, 26, 34, 39, 40). We attributed the increased energy expenditure to elevated UCP1 expression in iBAT of *Foxo1 KO^{Sf1}* animals. However, we do expect that other organs or tissues, such as muscle and heart, will play critical roles in regulating energy metabolism in the *Foxo1 KO^{Sf1}* mice, as they showed increased leptin sensitivity and glucose uptake. In this regard, more detailed approaches, including direct measurement of metabolic rates in individual organs, will be informative in future experiments.

Our current data are consistent with several additional lines of previously described evidence. First, mice lacking leptin receptors in VMH neurons display increases in body adiposity together with decreases in energy expenditure (12, 15). Second, removal of the catalytic PI3K subunit *Pik3ca* (p110α), an upstream molecule of FOXO1, from VMH SF-1 neurons results in increased sensitivity to HFD, due mainly to impaired energy expenditure (20). Third, VMH-specific SF-1 KO animals showed blunted energy expenditure in part due to impaired leptin action in the VMH (23). Finally, diet-induced increases in activation of PI3K lead to resistance to HFD-induced obesity in the SF-1$^{\Delta IR}$ animals, without changing energy expenditure, suggesting that deletion of IR in the SF-1 neurons is primarily related to PIP_3-mediated K_{ATP} channel modulation rather than the PI3K/pAkt/FOXO1 pathway (16).

The hyperinsulinemic-euglycemic clamp studies demonstrated that *Foxo1 KO^{Sf1}* animals have increased glucose uptake in heart and skeletal muscle, with comparable hepatic glucose production between genotypes. This is consistent with previous reports, in which the VMH is a critical site for the regulation of glucose uptake in peripheral tissues, including heart and skeletal muscle, primarily through the SNS (26, 34, 35, 41). Furthermore, several previous reports support our hypotheses that the deletion of FOXO1 in the VMH may lead to improved glucose homeostasis via changes in SNS signaling. For example, leptin injections into the

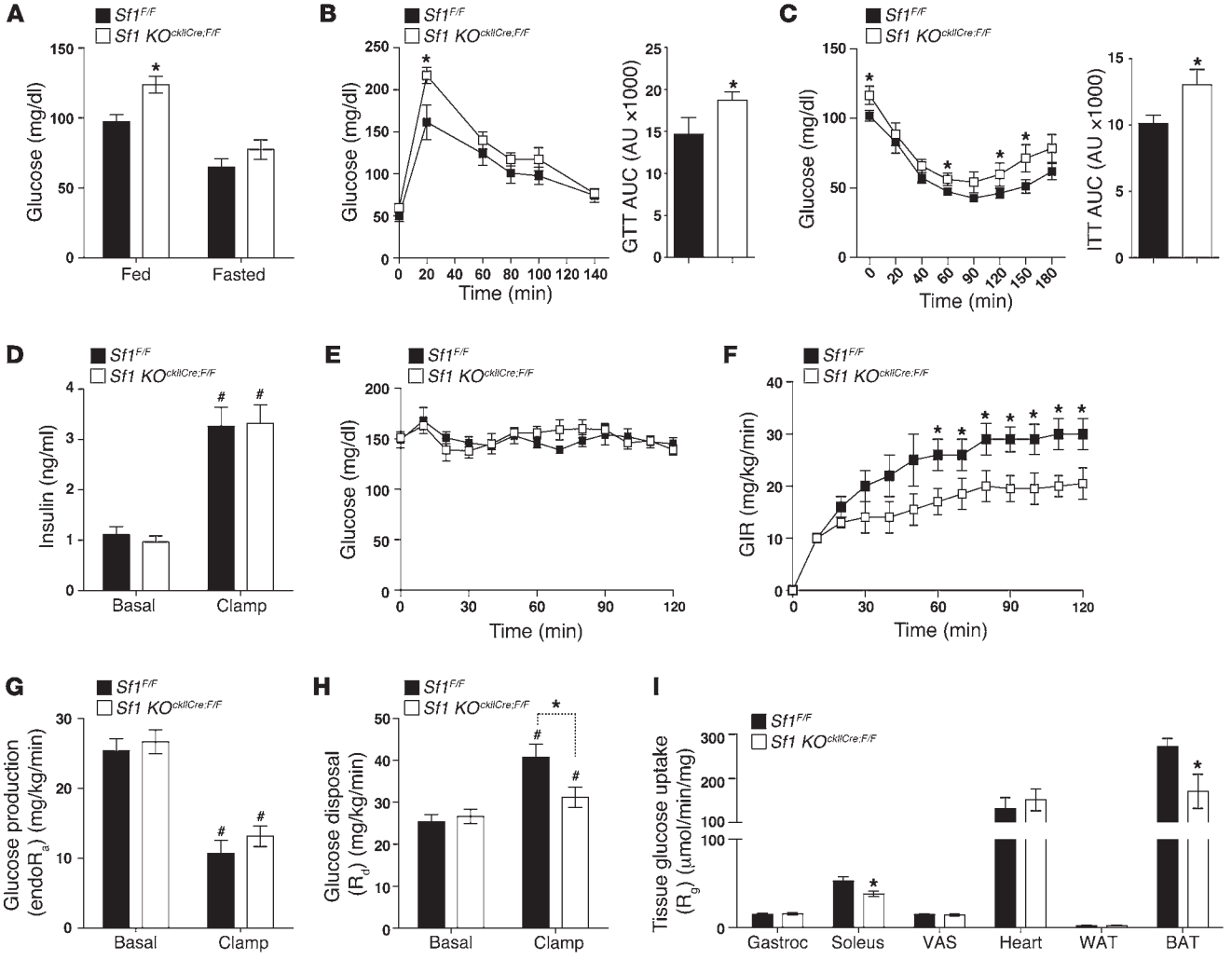

Figure 7

Effect of reduced SF-1 activity in the VMH on glucose and insulin homeostasis. (**A**) Glucose levels of NC-fed WT and *Sf1 KO*$^{cklCre;F/F}$ mice in fed and fasted states (male, 25–27 weeks old, n = 8–9/each genotype). (**B**) GTT and area under the curve (AUC) (male, 25–26 weeks old, n = 8–10/each genotype). (**C**) ITT and area under the curve (male, 26–27 weeks old, n = 8–10/each genotype). (**D**) Basal and clamped insulin, (**E**) blood glucose, (**F**) GIR, (**G**) hepatic $EndoR_a$, (**H**) R_d, and (**I**) tissue R_g in WT and *Sf1 KO*$^{cklCre;F/F}$ mice (n = 6–7 for each genotype). The data are expressed as mean ± SEM (*P < 0.05, #P < 0.01, Student's t test). VAS, vastus lateralis.

VMH preferentially increased glucose uptake in skeletal muscle, heart, and brown adipose tissue (BAT), and this increased glucose uptake was impaired when the SNS was denervated (26, 34, 42, 43). In addition, leptin receptor mutant mice that cannot activate STAT3 pathway exhibited only a modest defect in glucose homeostasis, despite the fact that the mutant animal showed the severe hyperphagia and obesity, suggesting that the leptin effect on glucose/insulin sensitivity may be differentiated from STAT3 pathways (40). Conversely, restoration of leptin receptors in the ARH and VMH of Kolesky rats (an animal model of mutated leptin receptors) using viral-mediated gene delivery improved glucose/insulin homeostasis. This effect was attenuated by applying PI3K inhibitors (24, 39, 44). Finally, leptin administration activates the SNS, and PI3K signaling is required for this effect (45). Collectively, these results indicate that leptin-mediated PI3K/pAkt/FOXO1 signaling in the VMH may play an important role, not only in mediation of sympathetic tone, but also in regulation of peripheral insulin action.

An intriguing finding of this study is that, whereas FOXO1 is involved in modulation of food intake through transcriptional regulation of NPY, AGRP, and POMC in the ARH, no clear difference in food intake was detected in *Foxo1 KO*^{Sf1} mice (2, 8). In addition, specific deletion of FOXO1 in ARH using POMC-Cre did not show any alternation in energy expenditure and peripheral glucose/insulin sensitivity (8). In contrast, deletion of FOXO1 in the VMH altered energy expenditure and whole-body glucose metabolism, without significant changes in food intake. Elucidation of a potential direct regulatory loop between FOXO1 and SF-1 provides evidence that FOXO1 and SF-1 direct a broad spectrum of transcriptional targets in VMH neurons. In this regard, we clearly do not expect that the SF-1 is the only target of FOXO1 in the VMH, and elucidation of additional transcriptional targets of FOXO1 is of great interest.

In summary, our data suggest that FOXO1 signaling in the VMH plays key roles in regulation of leptin sensitivity, energy expenditure, peripheral insulin action, and glucose homeostasis. These results support the idea that the VMH is a crucial hypothalamic site of whole-body metabolism and suggest that transcriptional programs regulated by FOXO1 are key in regulating energy balance and glucose homeostasis.

Methods

Animal care and generation of KO mice. Mice were kept at room temperature (22°C–24°C) with a 12-hour-light/dark cycle (lights on at 06:00), with normal mouse chow (NC; Teklad mouse/rat diet, no. 7001; 4.25% kcal from fat, 3.82 kcal/g) or HFD (Research Diet, no. D12331; 58% kcal from fat, 26% from sucrose, 5.56 kcal/g) and water provided ad libitum. To generate *Foxo1 KO^{Sf1}* mice, male mice homozygous for the floxed (F) *Foxo1* allele (21) and heterozygous for the *SF-1 cre* transgene (12, 20) were crossed with female mice homozygous for the floxed *Foxo1* allele. The littermate mice homozygous for the floxed *Foxo1* allele (*Foxo1$^{F/F}$*) served as controls (WT). All mice that performed experiments were on a mixed C57BL/6;129S6/SvEv background. To generate the *Sf1 KO$^{ckIICre;F/F}$* animals, we used same strategy described previously (23).

Immunohistochemistry. FOXO1 immunohistochemistry was performed on brain sections as previously described (23) using FOXO1-specific monoclonal antibody (Cell Signalling Technology, no. 2880). Briefly, mice were perfused with 10% neutral buffered formalin, and brains were postfixed with 10% formalin for 2 hours, cryoprotected in 20% sucrose overnight, and sectioned at 20 μm on a microtome. Sections were washed in PBS (pH 7.4) 3 times for 10 minutes each. Sections were preincubated with 0.3% H_2O_2 for 15 minutes and then permeabilized with 0.5% Triton X-100 in PBS for 20 minutes. To reduce nonspecific reactions, sections were treated with 1.5% normal serum from the species used to generate the secondary antibody. Sections were then incubated overnight at 4°C into 1:1,000 rabbit anti-FOXO1 primary antisera in PBT-azide containing 3% (w/v) normal donkey serum. Sections were then rinsed with PBS 6 times for 10 minutes each, incubated for 1 hour in 1:200 Alexa Fluor 488 goat anti-rabbit antibody (Invitrogen; A21206), rinsed 3 times in PBS, and mounted on gelatin-coated glass slides for visualization.

Metabolic cage studies. A combined indirect calorimetry system (CaloSys Calorimetry System, TSE Systems Inc.) was used for all metabolic studies. Experimental animals were acclimated for 6 days in a metabolic chamber with food and water. Room temperature for all metabolic studies was maintained at 22°C with a 12-hour-light/dark cycle. Airflow into the chamber was maintained at 0.6 l/min, and exhaust air from each chamber was measured for 3 minutes every 39 minutes. Heat generation, O_2 consumption, and CO_2 production were measured after acclimation, and the relationship between metabolic rate and body mass was normalized by using metabolic body size (body weight$^{0.75}$) if not specifically notified. During this time, ambulatory and rearing activities were also monitored with infrared beams.

Acute leptin administration. To assess the acute leptin effect, 6- to 7-week-old, body weight–matched male mice were acclimated in the metabolic chambers for 6 days with NC and water. Mice were given saline at 17:00 of experimental day 2, then leptin (5 mg/kg) was administered at 17:00 of experimental day 3 via i.p. injection. All the metabolic parameters, including body weight, meal size, meal frequency, and energy expenditure, were monitored during the experimental period using a combined indirect calorimetry system.

Twenty-four–hour fasting response. To measure acute (24-hour) fasting response in WT and *Foxo1 KO^{Sf1}* mice, body weight–matched (19.9 ± 0.4 g for WT and 19.4 ± 0.42 g for *Foxo1 KO^{Sf1}*), 4- to 5-week-old male mice were acclimated in the metabolic chambers for 6 days with NC and water. All food was removed between 16:30 and 17:00 at experimental day 3 and then refed after 24 hours. Metabolic parameters, including body weight, energy expenditure, and movement, were monitored during whole experimental procedures using a combined indirect calorimetry.

Body weight and composition. Body weight of WT and *Foxo1 KO^{Sf1}* (male and female) mice fed NC was monitored weekly from weaning (4 weeks old) to 12 to 13 weeks. In the HFD study, male WT and *Foxo1 KO^{Sf1}* mice were maintained on regular chow for 5 weeks and switched to HFD for an additional 6 weeks. The body fat composition of WT and *Foxo1 KO^{Sf1}* mice was determined using the Bruker Minispec mq10 NMR analyzer.

Hormone measurement. For corticosterone levels, we followed the protocol described elsewhere (20). Briefly, psychosocial stress was given to male mice by housing for 30 minutes in groups of 4 animals after 3-day isolation in individual cages. All blood samples for corticosterone measurement were taken by decapitation at indicated time frames (Supplemental Table 1), and the trunk blood was obtained. For FSH, LH, testosterone, T3, T4, epinephrine, and norepinephrine measurements, serum and/or plasma were obtained between 14:00 and 15:30. The blood samples for corticosterone, FSH, LH, and testosterone levels were sent to the Ligand Assay and Analysis Core at University of Virginia for measurement. For T3, T4, epinephrine, and norepinephrine, the plasma samples were sent to Hormone Assay and Analytical Services Core, Vanderbilt Diabetes Research and Training Center.

Protein and mRNA analyses. BAT samples were obtained for Q-PCR analysis. All BAT samples were collected between 13:00 and 15:00. Total RNA was isolated using TRIzol reagent (Invitrogen) and reverse transcribed with the SuperScript First-Strand Synthesis System (Invitrogen) for RT-PCR. Q-PCR was performed using an ABI 7900 HT Sequence Detection System (Applied Biosystems). Q-PCR primers used for the TaqMan method (Applied Biosystems) are as follows: 18S (ABI, Hs99999901) and UCP1 (ABI, Mm01244861).

For protein analysis, BAT from WT and *Foxo1 KO^{Sf1}* mice was homogenized in lysis buffer (Tris 20 mM, EDTA 5 mM, NP40 1% [v/v]) containing protease inhibitors (P2714-1BTL, Sigma-Aldrich), then resolved by SDS-PAGE, and finally transferred to a nitrocellulose membrane. After blocking the membrane with 5% nonfat milk, proteins (UCP1 and GAPDH) were detected using commercially available antisera (UCP1, Abcam; GAPDH, Santa Cruz Biotechnology Inc.).

VMH dissection and SF-1 levels. To measure mRNA and protein levels in the VMH of *Foxo1$^{F/F}$* and *Foxo1 KO^{Sf1}* male mice, mice were decapitated after deep anesthesia with i.p. injection of chloral hydrate (500 mg/kg). A coronal slice between bregma –1.22 mm and –2.06 mm was made, and then the VMH was microdissected with a scalpel under a microscope. All samples were immediately frozen to the dry ice. Total mRNAs were extracted from the sample of the VMH and used for Q-PCR analyses as described above. Q-PCR primers used for the TaqMan method are as follows: 18S (ABI, Hs99999901) and SF-1 (ABI, Mm03053390_s1). For SF-1 protein levels in the VMH, mice were fasted 24 hours, and the whole VMH tissue was dissected as indicated above and frozen immediately to the dry ice. Obtained brain tissues were ground and lysed in protein lysis buffer. After ultracentrifugation, samples were resolved by gradient (4%–12%) SDS-PAGE gel and transferred to a nitrocellulose membrane. Immunoblotting was performed with antiserum specific for SF-1 (46) and then visualized and analyzed using Li-COR Odyssey (Li-COR Inc.).

Gene profiling study. Total RNA was obtained from the VMH of WT and *Foxo1 KO^{Sf1}* mice using the RNeasy Lipid Tissue Mini Kit (Qiagen Sciences) and Phase Lock Gel (5 Prime Inc.). To make sure of reproducibility and biological significance, triple hybridizations were performed for each genotype with the RNA from 3 independent VMH samples, and each sample contained RNA from 3 animals (biological replicates). Genomics and Microarray Core Facility at UT Southwestern (http://microarray.swmed.edu/) checked RNA quality with a Bioanalyzer Chip (Agilent Technologies Inc.) and pro-

cessed the samples for hybridization with a Mouse-6 V2 BeadChip (Illumina Inc.). We used Partek Genomics Suite 6.5 (Partek Inc.) and Ingenuity Pathway Analysis (Ingenuity Systems Inc.) for data analysis and heat map generation. Expression results were deposited to the Gene Expression Omnibus (accession no. GSE36948; National Center for Biotechnology Information).

GTT, ITT, and hyperinsulinemic-euglycemic clamp study. GTTs were performed as described previously (15). For the FOXO1 KO model, male *Foxo1 KO^{Sf1}* mice and WT littermates aged 6–8 weeks (body weight, 24.94 ± 0.85 g for WT and 23.72 ± 0.81 g for *Foxo1 KO^{Sf1}*; $P > 0.1$) were fasted for 18 hours and provided water ad libitum. For the postnatal VMH-specific SF-1 KO model, 25- to 26-week-old male *Sf1 KO$^{ckIICre;F/F}$* mice and WT controls were used (body weight, 32.9 ± 1.7 g for WT and 32.26 ± 1.58 g for *Sf1 KO$^{ckIICre;F/F}$*; $P > 0.5$). After measurement of fasted glucose levels, the mice were administered glucose (1.5 g/kg body weight) i.p. Then, blood glucose levels were measured from bloods sampled from the tail nick at 20, 40, 60, and 90 minutes after injection. Blood glucose levels were determined by the glucose oxidase method using a commercial glucometer (Ascensia Contour, Bayer HealthCare).

For ITTs, 6- to 8-week-old male mice (body weight, 26.85 ± 0.52 g for WT and 26.32 ± 0.48 g for *Foxo1 KO^{Sf1}*; $P > 0.1$) or 26- to 27-week-old male mice (body weight, 34.9 ± 1.76 g for WT and 33.9 ± 0.62 g for *Sf1 KO$^{ckIICre;F/F}$*; $P > 0.5$) were fasted for 2 to 3 hours with water ad libitum. After measurement of basal levels of glucose, insulin (0.5 U/kg for FOXO1 model, 1 U/kg for SF-1 KO model; Eli Lilly and Company, HI-210) was administrated i.p. Blood glucose levels were monitored at given time points after insulin injection.

Hyperinsulinemic-euglycemic clamp study was performed as described elsewhere (22). Briefly, body weight– and body composition–matched WT and KO animals were anesthetized and surgically implanted with infusion catheters in the right jugular vein, tunneled subcutaneously, and exteriorized above the neck. After a 5-day recover period, mice were placed in a sterile shoe-box–sized mouse cage lined with bedding to begin a 4-hour fast. At $t = -120$ minutes, a primed, continuous infusion of [3-3H]glucose (2.5 μCi bolus plus 0.05 μCi/min) was initiated. At $t = -15$ and –5 minutes, blood samples were collected from the cut tail to measure basal glucose and insulin levels as well as to calculate the endogenous rate of glucose appearance (endoR_a) and disappearance (R_d). At $t = 0$ minutes, an insulin infusion (4 mU/kg/min) was used to induce hyperinsulinemia, and the infusion of [3-3H]glucose was increased to 0.1 μCi/min to account for changes in specific activity (SA). Blood samples were then taken every 10 minutes to assess blood glucose, and a variable GIR was adjusted to maintain target glycemic levels (150 mg/dl). Additional blood samples were taken every 10 minutes from $t = 80$–120 minutes to determine steady-state glucose turnover. At $t = 120$ minutes, a blood sample was taken to measure clamp insulin levels, and a 13 μCi bolus injection of 2-DG was administered to assess tissue-specific glucose uptake. Blood samples were taken at $t = 122$, 130, 137, and 145 minutes to measure plasma 2-DG specific activity. Glucose fluxes were calculated as previously described (22).

ChIP assay. The VMH were dissected as described above. A combined VMH sample from 5 different WT (*Foxo1$^{F/F}$*) mice was cross-linked by adding 1% formaldehyde to the sample after mincing the VMH tissue roughly into 1-mm pieces with a scalpel. The cross-linking was quenched after 10 minutes by adding 125 mM glycine. The tissue extracts were resuspended in SDS lysis buffer (1% SDS, 10 mM EDTA, 50 mM Tris [pH 8.1], 1 mM PMSF, 1 μg/ml aprotinin, 1 μg/ml pepstatin A), sonicated 10 times for 30 seconds with 2-minute interval time using Bioruptor$_{XL}$ (Diagenode), and then the lysates were cleared by centrifugation. The sonicated cell supernatant was diluted 10 fold in ChIP dilution buffer (0.01% SDS, 1.1% Triton X-100, 1.2 mM EDTA, 16.7 mM Tris-HCl [pH 8.1], 167 mM NaCl). After preclearance with protein A agarose/salmon sperm DNA (50% slurry) for 30 minutes at 4°C, 10% of precleared chromatin solution was saved for assessment of input chromatin. The rest of the chromatin solution was incubated with 2 different FOXO1 antibodies from other companies (Ab no. 1 from Cell Signaling Technology [no. 9454]; Ab no. 2 from Santa Cruz Biotechnology Inc. [sc-11350]) overnight at 4°C. After obtaining immune complex using protein A agarose/salmon sperm DNA beads, the complexes were washed 3 times with washing buffers as described in protocol (Millipore, no. 17-295). Complexes were then washed with 1× TE (pH 8.0) buffer, and histone complexes were eluted with freshly prepared elution buffer (1% SDS, 0.1 M $NaHCO_3$). The histone complexes were reversed by incubating at 65°C overnight, and the samples were purified after incubation with a buffer (10 μM EDTA, 40 μM Tris-HCl [pH 6.8], 2 μg proteinase K) at 45°C for 1 hour. The PCR reaction was performed using the following primers: *Sf1* forward, CCAAGGTCTCTCCAGTGCCT and, *Sf1* reverse, TTTCTCCTCCTTTGTTGGTG.

Cell culture and transfection. General cell culture conditions were previously described (47). Briefly, Neuro2A mouse neuroblastoma cells were maintained in MEM (Invitrogen) supplemented with nonessential amino acids, 10% FBS, and 100 U/ml penicillin/streptomycin (Invitrogen). Neuro2A cells were plated in 12-well plates at a density of 3×10^5 cells per well and cultured for additional 20–24 hours before transfection. Cells were transfected with Lipofectamine 2000 (Invitrogen) according to the manufacturer's instructions. Approximately 24 hours after transfection, cells were lysed and luciferase activity was determined using the Dual Luciferased Reporter Assay System (Promega) with the FLUOstar OPTIMA luminometer (BMG Labtech). All transfections were done in triplicate and repeated in 3 independent experiments. The 5′ proximal promoter region of the SF-1 mouse (–240 to +2) was amplified by PCR and cloned upstream of a luciferase reporter gene in pGL3-basic. To examine the role of 3 potential FOXO1-responsive elements, a deletion mutant spanning –80 to +2 was used. The PCR primers were 5′-GGGTCCCTGCCTCAGGCTCC-3′ for the –240, 5′-CACCAACAAAGGAGGAGAAA-3′ for the –80, and 5′-TCGTGGGTGGGGGGGCCACC-3′ for the +2.

Statistics. The data are represented as mean ± SEM as indicated in each figure legend. Statistical significance was determined by 2-tailed Student's *t* test, 1-way ANOVA, and 2-way ANOVA. GraphPad PRISM version 5.0a was used for the statistical analyses, and $P < 0.05$ was considered as a statistically significant difference.

Study approval. All experimental procedures were approved by the Institutional Animal Care and Use Committee at UT Southwestern.

Acknowledgments

We would like to thank Laura Brule, Mi Kim, Danielle Lauzon, Linh-An Cao, and the Mouse Metabolic Phenotyping Core at UT Southwestern (supported by P01 DK088761, PL1 DK081182, and UL1RR024923); Domenico Accili (Columbia University Medical Center, New York, New York, USA) for providing all the FOXO1 DNA constructs used for luciferase assays; and Syann Lee and Angie Bookout for helpful discussion. Data presented in this paper were also supported by the following: NIH grants R01DK53301 and RL1DK081185 and the American Diabetes Association to J.K. Elmquist, NIH grant R01HD061539 to C.F. Elias, and American Heart Association 11POST4880067 to K.W. Kim.

Received for publication January 12, 2012, and accepted in revised form April 18, 2012.

Address correspondence to: Joel K. Elmquist, UT Southwestern/Room Y6.322, 5323 Harry Hines Blvd., Dallas, Texas 75390-9077, USA. Phone: 214.648.2911; Fax: 214.648.5612; E-mail: joel.elmquist@utsouthwestern.edu.

1. Nakae J, et al. Regulation of insulin action and pancreatic beta-cell function by mutated alleles of the gene encoding forkhead transcription factor Foxo1. *Nat Genet*. 2002;32(2):245–253.
2. Kitamura T, et al. Forkhead protein FoxO1 mediates Agrp-dependent effects of leptin on food intake. *Nat Med*. 2006;12(5):534–540.
3. Ogg S, et al. The Fork head transcription factor DAF-16 transduces insulin-like metabolic and longevity signals in C. elegans. *Nature*. 1997; 389(6654):994–999.
4. Lin K, Dorman JB, Rodan A, Kenyon C. daf-16: An HNF-3/forkhead family member that can function to double the life-span of Caenorhabditis elegans. *Science*. 1997;278(5341):1319–1322.
5. Nakae J, Kitamura T, Kitamura Y, Biggs WH 3rd, Arden KC, Accili D. The forkhead transcription factor Foxo1 regulates adipocyte differentiation. *Dev Cell*. 2003;4(1):119–129.
6. Matsumoto M, Pocai A, Rossetti L, Depinho RA, Accili D. Impaired regulation of hepatic glucose production in mice lacking the forkhead transcription factor Foxo1 in liver. *Cell Metab*. 2007;6(3):208–216.
7. Kim MS, et al. Role of hypothalamic Foxo1 in the regulation of food intake and energy homeostasis. *Nat Neurosci*. 2006;9(7):901–906.
8. Plum L, et al. The obesity susceptibility gene Cpe links FoxO1 signaling in hypothalamic pro-opiomelanocortin neurons with regulation of food intake. *Nat Med*. 2009;15(10):1195–1201.
9. Cao Y, et al. PDK1-Foxo1 in agouti-related peptide neurons regulates energy homeostasis by modulating food intake and energy expenditure. *PloS One*. 2011;6(4):e18324.
10. Balthasar N, et al. Leptin receptor signaling in POMC neurons is required for normal body weight homeostasis. *Neuron*. 2004;42(6):983–991.
11. Scott MM, Williams KW, Rossi J, Lee CE, Elmquist JK. Leptin receptor expression in hindbrain Glp-1 neurons regulates food intake and energy balance in mice. *J Clin Invest*. 2011;121(6):2413–2421.
12. Dhillon H, et al. Leptin directly activates SF1 neurons in the VMH, and this action by leptin is required for normal body-weight homeostasis. *Neuron*. 2006;49(2):191–203.
13. King BM. The rise, fall, and resurrection of the ventromedial hypothalamus in the regulation of feeding behavior and body weight. *Physiol Behav*. 2006; 87(2):221–244.
14. Amir S. Intra-ventromedial hypothalamic injection of glutamate stimulates brown adipose tissue thermogenesis in the rat. *Brain research*. 1990; 511(2):341–344.
15. Bingham NC, Anderson KK, Reuter AL, Stallings NR, Parker KL. Selective loss of leptin receptors in the ventromedial hypothalamic nucleus results in increased adiposity and a metabolic syndrome. *Endocrinology*. 2008;149(5):2138–2148.
16. Klöckener T, et al. High-fat feeding promotes obesity via insulin receptor/PI3K-dependent inhibition of SF-1 VMH neurons. *Nat Neurosci*. 2011;14(7):911–918.
17. Minokoshi Y, Saito M, Shimazu T. Sympathetic denervation impairs responses of brown adipose tissue to VMH stimulation. *Am J Physiol*. 1986; 251(5 pt 2):R1005–R1008.
18. Rothwell NJ, Stock MJ. A role for brown adipose tissue in diet-induced thermogenesis. *Nature*. 1979; 281(5726):31–35.
19. Majdic G, et al. Knockout mice lacking steroidogenic factor 1 are a novel genetic model of hypothalamic obesity. *Endocrinology*. 2002;143(2):607–614.
20. Xu Y, et al. PI3K signaling in the ventromedial hypothalamic nucleus is required for normal energy homeostasis. *Cell Metab*. 2010;12(1):88–95.
21. Paik JH, et al. FoxOs are lineage-restricted redundant tumor suppressors and regulate endothelial cell homeostasis. *Cell*. 2007;128(2):309–323.
22. Hill JW, et al. Direct insulin and leptin action on pro-opiomelanocortin neurons is required for normal glucose homeostasis and fertility. *Cell Metab*. 2010;11(4):286–297.
23. Kim KW, et al. Steroidogenic factor 1 directs programs regulating diet-induced thermogenesis and leptin action in the ventral medial hypothalamic nucleus. *Proc Natl Acad Sci U S A*. 2011; 108(26):10673–10678.
24. Morton GJ, Gelling RW, Niswender KD, Morrison CD, Rhodes CJ, Schwartz MW. Leptin regulates insulin sensitivity via phosphatidylinositol-3-OH kinase signaling in mediobasal hypothalamic neurons. *Cell Metab*. 2005;2(6):411–420.
25. Scarpace PJ, Matheny M, Pollock BH, Tumer N. Leptin increases uncoupling protein expression and energy expenditure. *Am J Physiol*. 1997; 273(1 pt 1):E226–E230.
26. Toda C, et al. Distinct effects of leptin and a melanocortin receptor agonist injected into medial hypothalamic nuclei on glucose uptake in peripheral tissues. *Diabetes*. 2009;58(12):2757–2765.
27. Enriori PJ, Sinnayah P, Simonds SE, Garcia Rudaz C, Cowley MA. Leptin action in the dorsomedial hypothalamus increases sympathetic tone to brown adipose tissue in spite of systemic leptin resistance. *J Neurosci*. 2011;31(34):12189–12197.
28. Lowell BB, Spiegelman BM. Towards a molecular understanding of adaptive thermogenesis. *Nature*. 2000;404(6778):652–660.
29. Niijima A, Rohner-Jeanrenaud F, Jeanrenaud B. Role of ventromedial hypothalamus on sympathetic efferents of brown adipose tissue. *Am J Physiol*. 1984;247(4 pt 2):R650–R654.
30. Kageyama H, et al. Fasting increases gene expressions of uncoupling proteins and peroxisome proliferator-activated receptor-gamma in brown adipose tissue of ventromedial hypothalamus-lesioned rats. *Life Sci*. 2003;72(26):3035–3046.
31. Ahima RS, et al. Role of leptin in the neuroendocrine response to fasting. *Nature*. 1996;382(6588):250–252.
32. Fukuda M, et al. Monitoring FoxO1 localization in chemically identified neurons. *J Neurosci*. 2008;28(50):13640–13648.
33. Niswender KD, Morton GJ, Stearns WH, Rhodes CJ, Myers MG Jr, Schwartz MW. Intracellular signalling. Key enzyme in leptin-induced anorexia. *Nature*. 2001;413(6858):794–795.
34. Minokoshi Y, Haque MS, Shimazu T. Microinjection of leptin into the ventromedial hypothalamus increases glucose uptake in peripheral tissues in rats. *Diabetes*. 1999;48(2):287–291.
35. Ramadori G, et al. SIRT1 deacetylase in SF1 neurons protects against metabolic imbalance. *Cell Metab*. 2011;14(3):301–312.
36. Musatov S, et al. Silencing of estrogen receptor alpha in the ventromedial nucleus of hypothalamus leads to metabolic syndrome. *Proc Natl Acad Sci U S A*. 2007;104(7):2501–2506.
37. Rios M, et al. Conditional deletion of brain-derived neurotrophic factor in the postnatal brain leads to obesity and hyperactivity. *Mol Endocrinol*. 2001;15(10):1748–1757.
38. Buettner C, et al. Leptin controls adipose tissue lipogenesis via central, STAT3-independent mechanisms. *Nat Med*. 2008;14(6):667–675.
39. Morton GJ, Schwartz MW. Leptin and the central nervous system control of glucose metabolism. *Physiol Rev*. 2011;91(2):389–411.
40. Bates SH, Kulkarni RN, Seifert M, Myers MG Jr. Roles for leptin receptor/STAT3-dependent and -independent signals in the regulation of glucose homeostasis. *Cell Metab*. 2005;1(3):169–178.
41. Shiuchi T, et al. Hypothalamic orexin stimulates feeding-associated glucose utilization in skeletal muscle via sympathetic nervous system. *Cell Metab*. 2009;10(6):466–480.
42. Haque MS, Minokoshi Y, Hamai M, Iwai M, Horiuchi M, Shimazu T. Role of the sympathetic nervous system and insulin in enhancing glucose uptake in peripheral tissues after intrahypothalamic injection of leptin in rats. *Diabetes*. 1999;48(9):1706–1712.
43. Kamohara S, Burcelin R, Halaas JL, Friedman JM, Charron MJ. Acute stimulation of glucose metabolism in mice by leptin treatment. *Nature*. 1997; 389(6649):374–377.
44. Keen-Rhinehart E, Kalra SP, Kalra PS. AAV-mediated leptin receptor installation improves energy balance and the reproductive status of obese female Koletsky rats. *Peptides*. 2005;26(12):2567–2578.
45. Warne JP, et al. Impairment of central leptin–mediated PI3K signaling manifested as hepatic steatosis independent of hyperphagia and obesity. *Cell Metab*. 2011;14(6):791–803.
46. Kim KW, Jo YH, Zhao L, Stallings NR, Chua SC Jr, Parker KL. Steroidogenic factor 1 regulates expression of the cannabinoid receptor 1 in the ventromedial hypothalamic nucleus. *Mol Endocrinol*. 2008; 22(8):1950–1961.
47. Zhao L, et al. Central nervous system-specific knockout of steroidogenic factor 1 results in increased anxiety-like behavior. *Mol Endocrinol*. 2008; 22(6):1403–1415.